JOURNAL OF MATERIALS SCIENCE **37** (2002) 2475–2481

Microporosity formation in partially melted zone during welding of high nitrogen austenitic stainless steels

O. KAMIYA
Faculty of Engineering and Resources Science, Akita University, Japan

Z. W. CHEN
Faculty of Science and Engineering, Auckland University of Technology, New Zealand

Y. KIKUCHI
Joining and Welding Research Institute, Osaka University, Japan

Gas tungsten arc welding experiments were conducted using austenitic stainless steel containing 0.51%N and 0.78%N. Microstructure observation and hardness measurement were made to study the loss of nitrogen. It was found that welding resulted in a considerable loss of hardness in the weld metal for the case of 0.78%N steel, but not for 0.51%N steel. We explain this in terms of a higher nitrogen content enabling a significantly smaller critical pore size and hence N_2 porosity formation to be energetically more favourable. The major finding was that, for the case of 0.78%N steel, a band of microporosity was observed along and near the complete fusion boundary of the weld. It was identified that these micropores were present in the parent metal, not in the weld metal. Partial melting in the zone next to the complete fusion boundary resulted in a nitrogen content significantly higher than the solubility of nitrogen in the liquid channels or pockets. Nitrogen gas pores then formed and became trapped in that zone. Supporting this forming mechanism of microporosity band was the fact that hardness decreased in that zone due to the loss of nitrogen in γ phase matrix for solute strengthening and that nitride particles disappeared after welding.

1. Introduction

Addition of nitrogen, up to 1%, to austenitic stainless steels significantly improves their strength, corrosion properties and austenitic stability [1–3]. Hence, these high nitrogen steels (HNS) are increasingly finding wider industrial application in recent years [1–4] and have been considered as structural materials for fusion reactors in Japan. For these steels to be used for structural purposes, weldability is an important consideration. Welding can cause the formation of N_2 pores, lowering the amount of dissolved nitrogen for solute strengthening and other beneficial effects.

Hence, nitrogen loss and porosity formation in weld metal have been the major concerns of HNS welding [5–8]. Hertzman *et al*. [5, 7] showed that plasma enhanced the nitrogen intake in the weld metal. Vilpas and Hanninen [9] also reported that the addition of N_2 in Ar shielding gas increased the nitrogen content of the weld pool. Despite of these studies, Gavriljuk and Berns [3] recently concluded that little is known about the effect of welding procedures and parameters on the nitrogen content in the weld pool.

As part of a research effort on HNS to be used as structural materials for fusion reactors, we have been conducting studies to understand the weldability of these steels [10–12]. In this paper, we present our observation on the formation of microporosity in the partially melted zone (PMZ) during gas tungsten arc (GTA) welding. Hardness data to relate the changes of nitrogen content in weld metal and in PMZ will also be presented. Based on these, mechanisms of the microporosity formation and nitrogen loss are suggested.

2. Experimental procedures

To obtain high nitrogen content in steel to service as the parent metal, we first made large welds using GTA welding technique at high nitrogen pressures inside a pressure chamber. Subsequently, weld beads were made on each of the high nitrogen weld sample outside the pressure chamber. The welding sequence is schematically shown in Fig. 1. The compositions of the original base metal and the filler wire were given in Table I. Welding at high nitrogen pressures and the analysis for nitrogen content have been described elsewhere [10–12]. Two levels of nitrogen were used in the present work and they were 0.51% (wt% throughout) and 0.78% obtained by welding at 4.0 and 6.1 MPa N_2 pressure, respectively, inside the chamber.

For the welds subsequently made outside the chamber, no filler wire was used, meaning that the welds were

TABLE I Chemical composition (wt%) of the 316L type steel plate and weld wire used in the present study

	C	Si	Mn	P	S	Ni	Cr	Mo	Fe
316L plate	0.015	0.68	1.24	0.032	0.003	12.17	17.26	2.07	Bal.
316L wire	0.024	0.44	1.63	0.017	0.005	12.51	18.92	2.40	Bal.

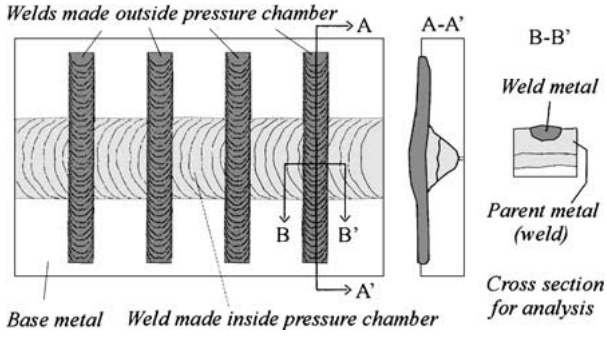

Figure 1 Schematic showing a large weld bead first made inside the high N_2 pressure chamber and welds on the same plate subsequently made at atmospheric pressure outside the chamber.

made simply by GTA remelting. The tip of the 2 mm diameter electrode was sharpened for every weld. Welding current at 150 A and a 2 mm electrode-work gap were the same for all the welds. Welding speeds were 3.3 mm/s and 1.7 mm/s. Industrial pure Ar and N_2 as were used as shielding gases. Welding voltages were automatically adjusted to 12 V and 18 V, respectively, for Ar and N_2 gases.

Metallographic samples were taken as illustrated in Fig. 1. The final weld is simply referred to as weld metal. The weld made inside the pressure chamber was to obtain high nitrogen contents and will be referred hereafter to as parent metal. The sectioned samples were mounted, polished and etched following the normal metallography procedure. Hardness measurement of unetched samples was made using a Vickers micro-hardness tester. Unetched samples were also examined using a Leisa scanning electron microscope (SEM) and the microconstituents were analysed by energy-dispersive spectroscopy (EDS) with 10 kV accelerating voltage.

3. Results

3.1. Weld microstructure

Welds made using the 0.51%N parent metal were largely free of porosity. An example is shown in Fig. 2, where the boundary between the weld metal and the parent metal is not very obvious in this polished but unetched sample. On the contrary, when the 0.78%N parent metal was used, micropores were observed to be present along and near the fusion boundary. An example of this is illustrated in Fig. 3.

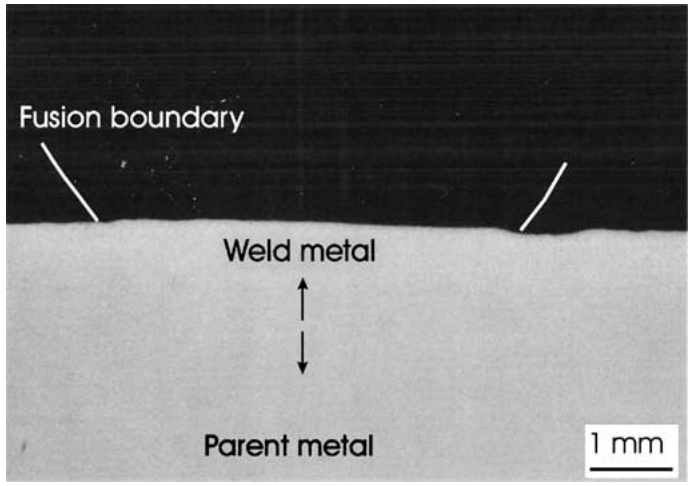

Figure 2 Optical micrograph of a polished sample of the weld made using 0.51%N parent metal, Ar shielding gas and 3.3 mm/s travel speed.

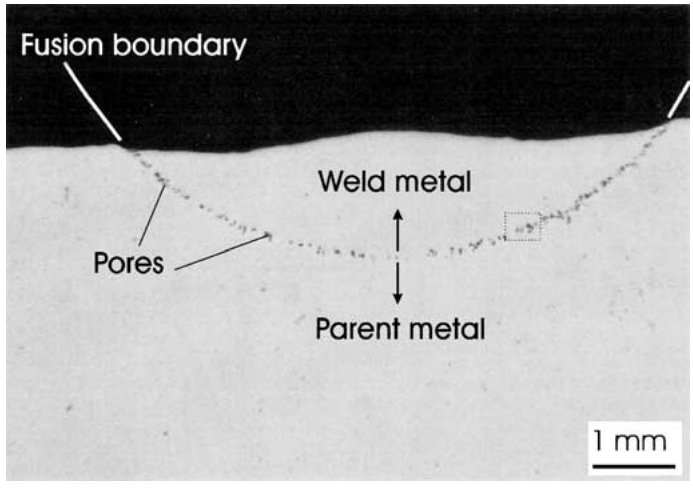

Figure 3 Optical micrograph of a polished sample of the weld made using 0.78%N parent metal, Ar shielding gas and 3.3 mm/s travel speed (Micropores are observed along the whole fusion boundary).

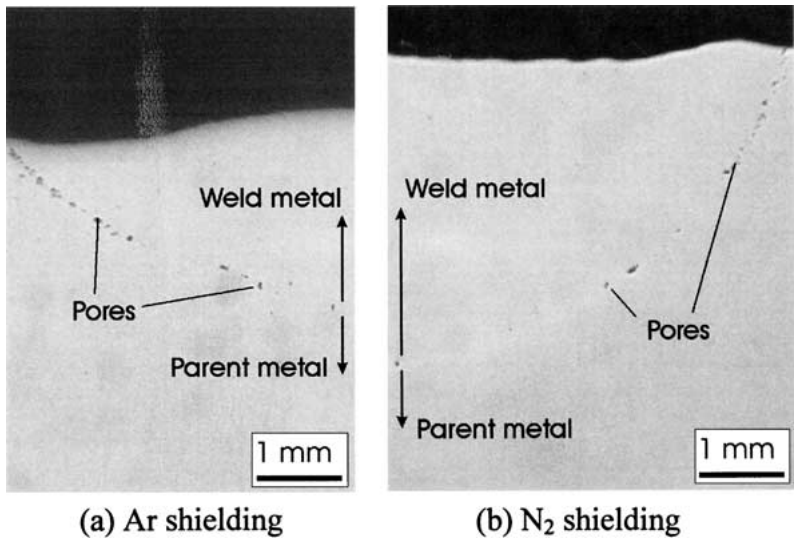

Figure 4 Optical micrograph of polished samples (half cross-section for each weld) of the weld made using 0.78%N parent metal and 1.7 mm/s travel speed: (a) Ar shielding and (b) N_2 shielding (Micropores are observed along the fusion boundary).

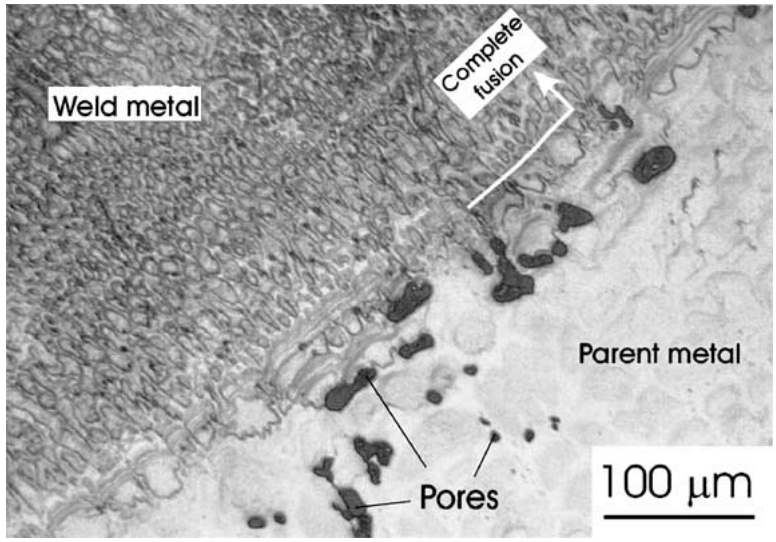

Figure 5 Optical micrograph (higher magnification) of an etched sample of the weld made using 0.78%N parent metal, Ar shielding gas and 3.3 mm/s travel speed, showing that micropores are within the "parent metal".

These fusion boundary micropores were observed for all the high nitrogen welds sampled (totalling eight). Further examples are given in Fig. 4. With the same shielding condition (Ar), comparing Fig. 4a to Fig. 3, a lower welding speed resulted in a larger weld bead but the shape remained unchanged. However, when N_2 shielding was used, which was associated with a higher voltage, a considerably deeper penetration was achieved (Fig. 4). In general, the amount of pores appeared to be less for the case of N_2 shielding. Quantitatively, the porosity level was not determined.

The more precise locations of these micropores were revealed in higher magnifications after etching the samples, as shown in Fig. 5. Surprisingly, these pores were not present in the weld metal. Weld metal could be identified starting as fine grains grown perpendicularly from the complete fusion boundary. As shown in Fig. 5, micropores were clearly seen in the parent metal adjacent to the complete fusion boundary. They could be found up to $\sim$150 μm away from that boundary. As is also shown in Fig. 5, micropores were likely present in the interdendritic regions. This is particularly apparent for the small size pores.

Within the band of the micropores, moving more towards the fusion boundary, not only the pore sizes were larger but also less and less fine particles were present. This is illustrated in Fig. 6 by SEM micrographs. Next to the fusion boundary (Fig. 6a) was a single γ-phase only, plus micropores. On the other hand, near the edge of the microporosity band, meaning more inside the parent metal, fine particles could be clearly observed (Fig. 6b). An EDS analysis is given in Fig. 7, showing that the particles contain a high nitrogen content and a comparatively higher chromium content. Hence, these particles are likely to be the known phase Cr_2N, although as shown in Fig. 7 they contain other elements.

3.2. Hardness

Data of micro-hardness of the welds are plotted as a function of distance, starting from the central top

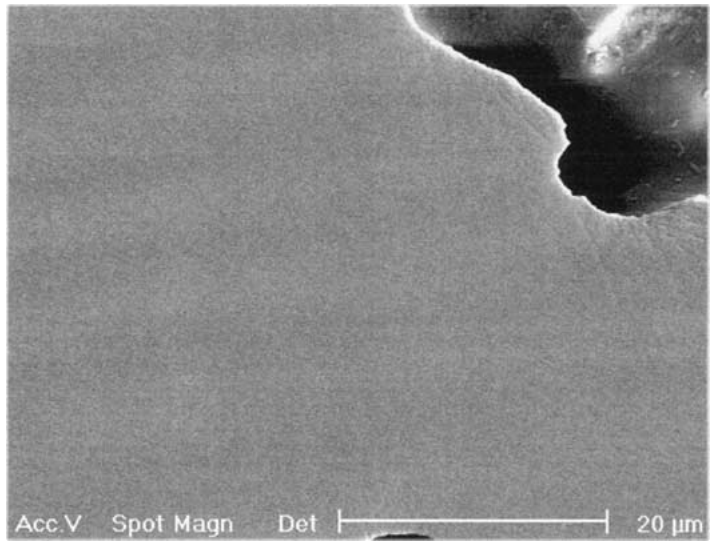

(a)

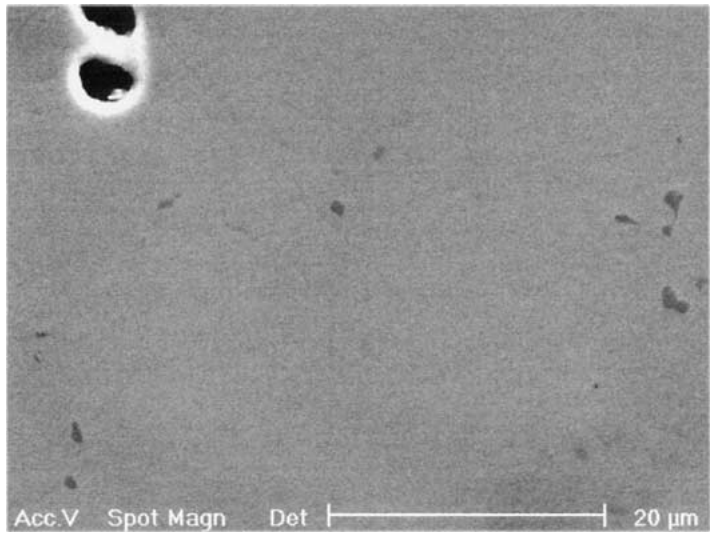

(b)

Figure 6 SEM micrographs of a polished sample of the weld using 0.78%N parent metal, N_2 shielding gas and 1.7 mm/s travel speed: (a) inside the microporosity (partially melted) zone but close to the complete fusion boundary (CFB), showing single γ phase, and (b) on the edge of the zone (no more pores, after the two pores top left, moving inside the parent metal), showing small and dark particles.

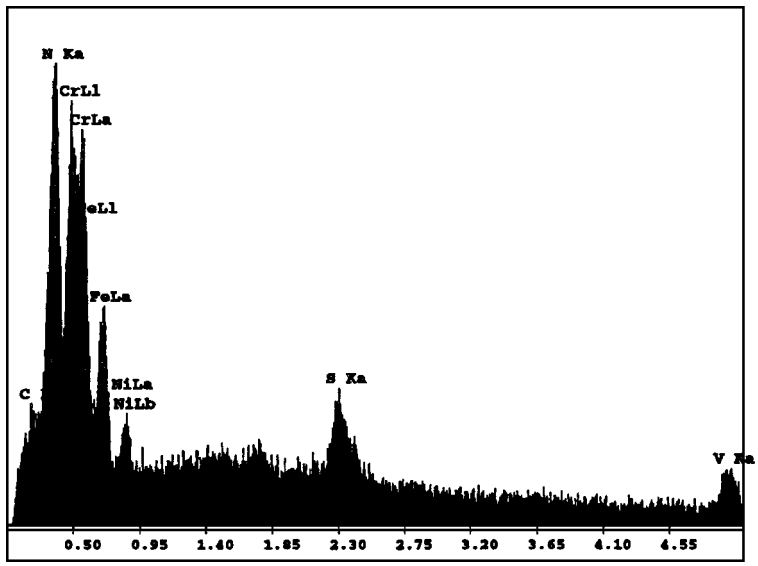

Figure 7 EDS spectrum of a particle as those shown in Fig. 6 (full scale CPS = 685).

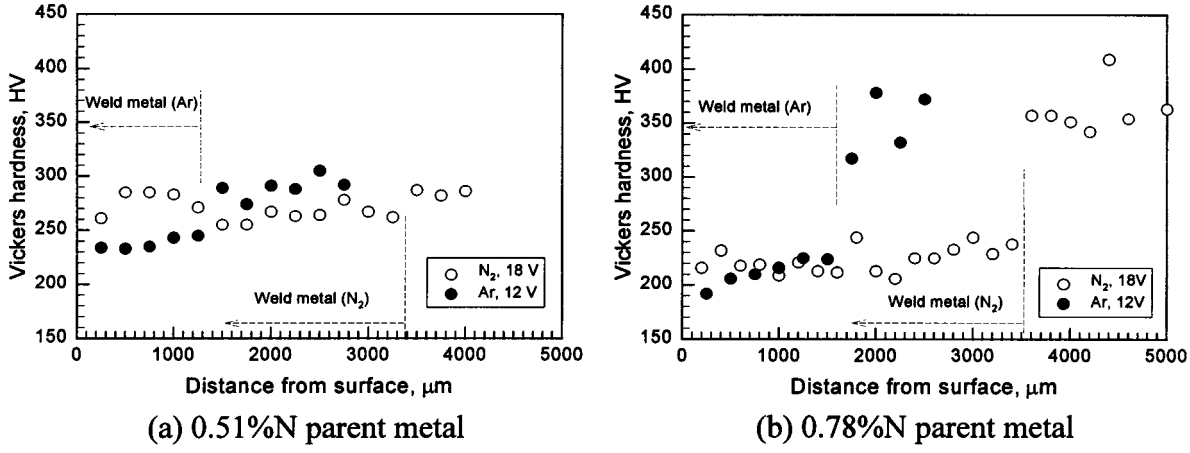

Figure 8 Variation of hardness from weld metal to parent metal of welds made with 3.3 mm/s travel speed: (a) 0.51%N parent metal and (b) 0.78%N parent metal.

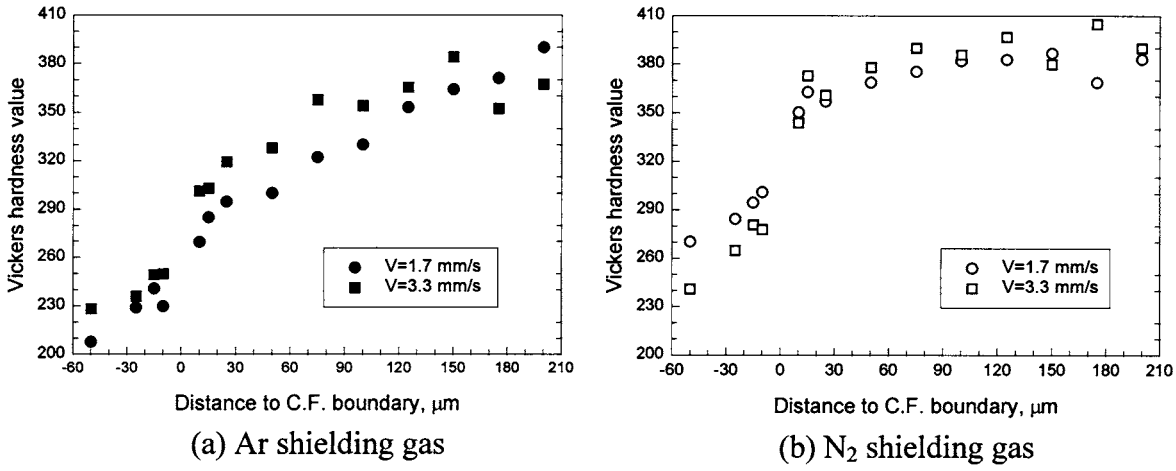

Figure 9 Variation of hardness mainly in the regions across the complete fusion (C.F.) boundary of the weld made using 0.78%N parent metal with travel speed as indicated. In most cases, each value is the average of three measurements: (a) Ar shielding gas and (b) N_2 shielding gas.

surface of the welds and down to the parent metal, in Fig. 8a and b for 0.51%N and 0.78%N content, respectively. For the case of 0.51%N (Fig. 8a), when Ar shielding was used, hardness values in the weld metal (230–240 HV) could be observed slightly lower than that in the parent metal (270–300 HV). However, when N_2 shielding gas was used, hardness in the weld metal did not decrease significantly.

On the other hand, a very large decrease in hardness (from 350–400 HV to 200–230 HV) was observed when 0.78%N steel was used. Furthermore, this large decrease was not affected significantly by the different use of shielding gas (Fig. 8b). It is noted that the hardness values of the weld metal were lower in the case of higher nitrogen parent metal (Fig. 8b) than those in the weld metal made using the lower nitrogen parent metal (Fig. 8a). This is despite the significantly harder parent metal which is associated with the higher nitrogen content.

A closer examination of the hardness change near the complete fusion boundary for the 0.78%N steel is presented in Fig. 9. It is clear that, adjacent to the boundary, hardness of parent metal decreased towards the boundary. For the case of Ar shielding gas, hardness decreased to a value estimated to be ~270 HV. On the other hand, this value was significantly higher, estimated to be ~330 HV for the case of N_2 shielding. Furthermore, the width within which hardness decreased in the parent metal is estimated to be ~150 μm for the case of Ar, significantly higher than that estimated to be ~70 μm for the case using N_2.

4. Discussion

4.1. Porosity formation and nitrogen loss

It has been known that gas pores can form in weld metal during welding of HNS [5, 6, 8]. Pore formation is a complex phenomenon, particularly so given the uncertainty of partitioning of gases in a plasma environment. In the following, the decrease in nitrogen solubility with the increase in temperature, both in solid and in liquid states, is used to thermodynamically explain the formation of porosity. For the excessive nitrogen dissolved in liquid metal to form gas pores through the reaction:

$$N(\%) \rightarrow \frac{1}{2}\mathrm{N_2(gas)} \tag{1}$$

the pressure inside a N_2 gas pore, according to Sievert's law, is:

$$P_{\mathrm{N_2}} = \left[\frac{N(\%)}{K}\right]^2 \tag{2}$$

where $N(\%)$ is the nitrogen concentration in liquid, K is the equilibrium constant. The condition for a gas pore to form is:

$$P_{N_2} \geq P_C = P_a + P_m + P_\sigma = P_a + \rho_l g h + \frac{2\sigma_{lg}}{r} \quad (3)$$

where P_C, P_a, P_m, P_σ, ρ_l, g, h, σ_{lg} and r are the critical pressure, ambient pressure, metallostatic pressure, surface tension pressure (due to the Gibbs-Thompson effect), density of the liquid, acceleration of gravity, distance from the surface of the liquid, surface tension between the liquid and gas, and radius of the pore, respectively.

Solubility data determined by Kikuchi *et al.* [13] for Fe-18Cr-8Ni, which show a general trend of decrease in nitrogen solubility as temperature increases, is suitable to approximately predict the solubility of nitrogen in our steel. Our steel contained molybdenum which should increase the nitrogen solubility slightly, but higher nickel in our steel should slightly decrease the solubility. From Kikuchi's data, the solubility of nitrogen should be ~0.3N% at the melting temperatures and this value only changes slightly from solid to liquid. As the nitrogen contents of the starting parent metals were higher than that solubility value, N_2 gas pores could form during the melting stage of welding, if Equation 3 is satisfied.

In using Equation 3, we take: $P_a = 1$ atm, $h_{max} = 0.005$ m, $\sigma_{lg} = 1.32$ N/m [14]. Then the equation becomes:

$$P_{N_2} \geq 1 + 0.0038 + \frac{2.6 \times 10^{-5}}{r} \text{ atm} \quad (3a)$$

The temperature of the weld pool is, for an approximation, assumed to be ~2000 K and not to change considerably. Then the solubility should be ~0.2% [13]. Hence, from Equation 2, we have $K \cong 0.2$. The maximum obtainable values of P_{N_2} is then calculated to be 15.2 atm for 0.78%N and 6.5 atm for 0.51%N. Then from Equation 3a, the critical values of pore radii are $r = 2.4 \times 10^{-6}$ m $= 1.8\ \mu$m for 0.78%N and $r = 4.7 \times 10^{-6}$ m $= 4.7\ \mu$m for 0.51%N. The ratio of the radii is:

$$\frac{r_{0.51\%N}}{r_{0.71\%N}} = 2.6$$

The growth of a pore, once it reaches the critical size, is much easier as the surface tension pressure decreases with the further growth. Hence, it may be suggested that the considerable loss of nitrogen, for the case of 0.78%N as in Fig. 8, was due to porosity formation. On the other hand, the critical pressure may have been too high for pores to reach the critical size for stable growth, in the case of 0.51%N. Furthermore, a higher nitrogen content should, in general, provide a higher diffusion flux of nitrogen to a pore surface for a pore to reach the critical size.

If porosity formation was difficult, then the major mechanism for nitrogen loss did not operate. This might explain the higher hardness of the weld metal for the case of 0.51%N (Fig. 8a), in comparison to that of 0.78%N (Fig. 8b). Gas pores generated in molten state during welding could float to the surface of the melt and escape. However, unfavourable weld pool convention [15] and fast cooling could result in gas pores being trapped after solidification. Gas pores present in the weld metal of HNS welds have been known [5, 6, 8] and also found in our weld samples [16], although these pores were not always observed in a two dimensional cross section.

Another way of losing nitrogen during welding is through the reaction (Equation 1) on the surface. This should largely depend on the partial pressure of nitrogen in the shielding atmosphere. For N_2, there should be a certain solubility of nitrogen in the melt (~0.2%). For Ar shielding, on the other hand, the partial pressure of N_2 was zero, meaning no solubility. Hence, the driving force for the reaction should be higher. The surface reaction mechanism was probably the only one applied to the case of 0.51%N steel. This may explain that the hardness of the 0.51%N weld only decreased to 230–240 HV (Fig. 8a), not to ~210 HV (Fig. 8b). In the case of N_2 shielding, the driving force for reaction (Equation 1) on the weld pool surface must be significantly lower and hence the loss of nitrogen was very little (Fig. 8a).

4.2. Micropores in partially melted zone (PMZ)

To explain our finding of micropores present in the parent metal adjacent to the complete fusion boundary, but not the weld metal, the metallurgical change in that zone during welding needs to be considered. The parent metal solidified previously during welding in the high N_2 pressure chamber and the microstructure was primarily γ-phase dendrites but some Cr_2N phase particles were present along the interdendritic regions and grain boundaries [11]. When temperature increases, the equilibrium melting reaction and the approximate temperature range, based on the thermodynamic database THERMOCAL, should be:

$$\gamma + Cr_2N \rightarrow \text{Liq. at } 1591 \text{ K}$$

$$\gamma \rightarrow \text{Liq. from } 1591 \text{ K to } 1695 \text{ K, i.e., } \Delta T = 104 \text{ K}$$

In regard to melting and solidification during welding, discussion can be made with reference to Fig. 10, focusing on the zone near the complete fusion boundary. During welding, the temperature of the complete fusion boundary should be at ~1695 K. PMZ started at the complete fusion boundary where $f_s = 0$ and f_s increased in the direction towards the parent metal (moving left in Fig. 10). f_s became 1 at the location where temperature was just below 1591 K. In PMZ, N_2 pores formed when solid of high nitrogen content became liquid of lower nitrogen solubility, in a similar way as previously discussed.

It is expected that nitrogen content is higher in the γ phase more towards the interdendritic regions and grain boundaries. Some Cr_2N phase particles are also present in those regions and boundaries. These higher nitrogen content regions and phases should melt first during

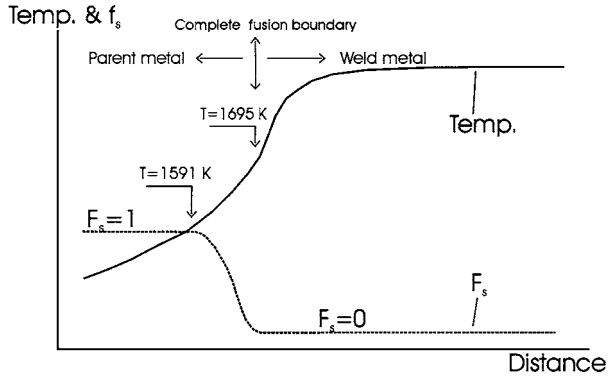

Figure 10 Schematic illustration of a temperature distribution and the corresponding solid fraction during welding.

welding, resulting in a nitrogen content higher than the nominal value and hence in the formation of porosity in the interdendritic liquid channels, grain boundaries and pockets. If these pores could not escape through the solid skeletons or pockets in the PMZ, they were then trapped in that zone, as shown in Figs 3–5.

The degree of melting was higher towards the complete melting boundary, and hence more pores formed near that boundary were expected. Accompanying this was the complete loss of Cr_2N near the boundary, as in Fig. 6a. Moving away from the boundary in the porosity band, pores became less and smaller as the result of less melting. Hence, nitride particles could be observed in this region (Fig. 6b). Although the melting reaction $\gamma + Cr_2N \rightarrow$ Liq. should take place in the entire PMZ, the rate of the reaction increased with overheating ($\Delta T = T - 1591$ K), which was higher towards the complete fusion boundary.

Formation of micropores means a loss of nitrogen in the resolidified γ matrix, hence lowering the hardness. Hence, within the PMZ and moving closer to the boundary, a larger decrease in hardness was also to be expected, as was the case shown in Fig. 9a. A further support of the suggested porosity forming mechanism is the width of microporosity band at about 150 μm (see Fig. 5) to be consistent with the width of hardness affected zone determined also to be about 150 μm (Fig. 9a), for the case of Ar shielding.

5. Conclusions

The loss of nitrogen in high nitrogen austenitic steels during welding depended on the original nitrogen contents. At 0.51%N, welding did not result in a very high loss of nitrogen. At 0.78%N, hardness of the weld metal decreased considerably due to the loss of nitrogen. The explanation for this is that the high nitrogen content has enabled a significantly smaller critical pore size and hence N_2 porosity formation to be energetically more favourable, resulting in the significant loss of nitrogen for the case of 0.78%N steel.

For the 0.78%N steel, we have observed the formation of microporosity which was not present in the weld metal but was in the PMZ of the parent metal. Partial melting in that zone resulted in a nitrogen content significantly higher than the solubility of nitrogen in the liquid channels or pockets. Nitrogen gas pores then formed and became trapped in that zone. This forming mechanism of microporosity was supported by the hardness values which decreased and by the disappearance of nitride particles in that zone.

Acknowledgements

The authors are very grateful for the support given to them by Mr. R. Kato and Mr. F. Ashihara of Akita University, Mr. R. Thompton of the Auckland University of Technology, Mr. S. Strover, Professor W. Gao, Dr. J. T. Gregory, Mr. D. Stringer and Ms Y. Jing of the University of Auckland and Mr M. Ogawa of The National Institute for Materials Science, Japan.

References

1. G. STEIN, I. HUCKLENBROICH and H. FEICHTINGER, *Mater. Sci. Forum* **318–320** (1999) 151.
2. M. LIJAS and J. O. NILSSON, *ibid.* **318–320** (1999) 189.
3. V. G. GAVRILJUK and H. BERNS, in "High Nitrogen Steels" (Springer, New York, 1999).
4. J. SUNDVALL, J. OLSSON and B. HOLMBERG, *Mater. Sci. Forum* **318–320** (1999) 181.
5. S. HERTZMAN and S. WESSMAN, *ibid.* **318–320** (1999) 579.
6. M. HARZENMOSER, C. RENNHARD, M. HERETH and M. DIENER, *ibid.* **318–320** (1999) 591.
7. S. HERTSMAN, R. F. A. JARGELIUS PETTERSSON, R. BLOM, J. ERIKSSON and E. KIVINEVA, *ISIJ International* **36** (1996) 968.
8. V. GROB, H. HEUSER and T. LADWEIN, *Mater. Sci. Forum* **318–320** (1999) 597.
9. M. VILPAS and HANNINEN, *ibid.* **318–320** (1999) 603.
10. Y. KIKUCHI, F. MATSUDA, T. OKABE and M. OHTA, *ISIJ International* **36** (1996) 977.
11. O. KAMIYA and Y. KIKUCHI, *Mater. Sci. Forum* **318–320** (1999) 609.
12. Y. KIKUCHI, O. KAMIYA and H. KOBAYASHI, *ibid.* **318–320** (1999) 621.
13. M. KIKUCHI, M. KAJIHARA and K. FRISK, in Proceedings of the International Conference on High Nitrogen Steels, Institute of Metals, 1989, p. 7.
14. M. INAGAKI, in "Stainless Steel Handbook" edited by M. Hasegawa (Nikkan Kogyo, Japan, 1985) p. 732.
15. S. KOU, in "Welding Metallurgy" (John Wiley & Sons, New York, 1987) p. 102.
16. O. KAMIYA, Y. KIKUCHI and Z. W. CHEN, in Proceedings of the International Conference on Processing and Manufacturing of Advanced Materials (Elsevier Science, 2001).

Received 4 June 2001
and accepted 13 February 2002